



USGS Patuxent Wildlife Research Center

From the Selected Works of Neal Woodman

2013

Morphological distinctiveness of Javan *Tupaia hypochrysa* (Scandentia, Tupaiidae)

Eric J. Sargis
Neal Woodman
Natalie Morningstar
Aspen Reese
Link E. Olson



Available at: <https://works.bepress.com/nw/22/>

Morphological distinctiveness of Javan *Tupaia hypochrysa* (Scandentia, Tupaiidae)

ERIC J. SARGIS,* NEAL WOODMAN, NATALIE C. MORNINGSTAR, ASPEN T. REESE, AND LINK E. OLSON

Department of Anthropology, Yale University, P.O. Box 208277, New Haven, CT 06520, USA (EJS, NCM)

Department of Ecology and Evolutionary Biology, Yale University, P.O. Box 208106, New Haven, CT 06520, USA (EJS, ATR)

Division of Vertebrate Zoology, Yale Peabody Museum of Natural History, New Haven, CT 06520, USA (EJS, ATR)

United States Geological Survey, Patuxent Wildlife Research Center, National Museum of Natural History,

Smithsonian Institution, Washington, DC 20013, USA (NW)

University of Alaska Museum, University of Alaska Fairbanks, Fairbanks, AK 99775, USA (LEO)

* Correspondent: eric.sargis@yale.edu

The common treeshrew, *Tupaia glis*, represents a species complex with a complicated taxonomic history. It is distributed mostly south of the Isthmus of Kra on the Malay Peninsula and surrounding islands. In our recent revision of a portion of this species complex, we did not fully assess the population from Java (*T. “glis” hypochrysa*) because of our limited sample. Herein, we revisit this taxon using multivariate analyses in comparisons with *T. glis*, *T. chrysogaster* of the Mentawai Islands, and *T. ferruginea* from Sumatra. Analyses of both the manus and skull of Javan *T. “glis” hypochrysa* show it to be most similar to *T. chrysogaster* and distinct from both *T. glis* and *T. ferruginea*. Yet, the Javan population and *T. chrysogaster* have different mammae counts, supporting recognition of *T. hypochrysa* as a distinct species. The change in taxonomic status of *T. hypochrysa* has conservation implications for both *T. glis* and this Javan endemic.

Key words: cranium, digits, hand, mandible, manus, postcranium, rays, skeleton, skull, treeshrews

© 2013 American Society of Mammalogists

DOI: 10.1644/13-MAMM-A-042.1

Treeshrews (order Scandentia) are superficially squirrel-like mammals that inhabit tropical forests throughout much of South and Southeast Asia. Despite the former inclusion of treeshrews in the order Primates (Carlson 1922; Napier and Napier 1967), the taxonomy of Scandentia has been neglected and has not been formally revised since Lyon’s (1913) monographic study 100 years ago. One particularly problematic species complex is *Tupaia glis* (Diard, 1820), the common treeshrew, which has recently included as many as 27 synonyms (Helgen 2005). This “wastebasket” taxon was once considered to be widespread, ranging through the Malay Peninsula to Sumatra and Borneo, but our recent taxonomic revision (Sargis et al. 2013) restricted its distribution to the Malay Peninsula and surrounding islands south of the Isthmus of Kra (Fig. 1).

We recently analyzed the proportions of hand (manus) bones in several populations of *T. glis* using the methodology developed by Woodman and colleagues to distinguish “cryptic” soricid species (Woodman and Morgan 2005; Woodman 2010, 2011; Woodman and Stephens 2010), and it illustrated the effectiveness of this approach for distinguishing

similarly cryptic treeshrew species (Sargis et al. 2013). In that study, we investigated the manus morphology of *T. “glis” hypochrysa* from Java but were hampered by having only a single specimen available to us. This limited our ability to draw firm conclusions regarding the distinctiveness of this taxon, despite the clear differentiation of that individual from other taxa in our analyses (Sargis et al. 2013).

Tupaia “glis” hypochrysa was originally described as *T. ferruginea hypochrysa* Thomas, 1895, but was later elevated to *T. hypochrysa* by Lyon (1913), who included it with *T. chrysogaster* Miller, 1903, the golden-bellied treeshrew (from the Mentawai Islands off the west coast of Sumatra; Fig. 1), in his “Hypochrysa Group.” Chasen (1940) synonymized *T. hypochrysa* with *T. glis*, a decision followed in subsequent classifications (Honacki et al. 1982; Wilson 1993; Helgen 2005). Our preliminary results suggested that the Javan population could be distinct from *T. glis*, *T. chrysogaster*,



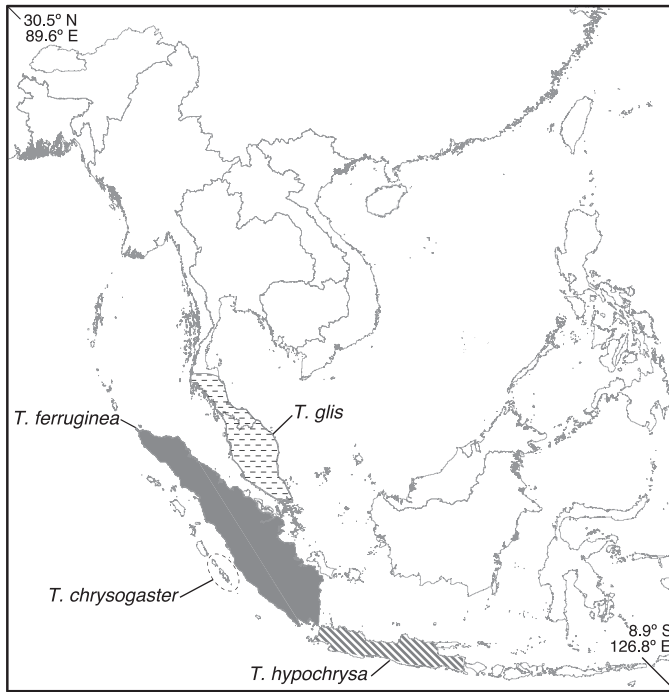


FIG. 1.—Map of Southeast Asia showing approximate ranges of the treeshrews *Tupaia chrysogaster*, *T. ferruginea*, *T. glis*, and *T. hypochrysa*. Map redrawn from Roberts et al. (2011: fig. 1) and Lyon (1913:75).

and *T. ferruginea* Raffles, 1821 from Sumatra (Sargis et al. 2013). Here, we test that hypothesis by using both an expanded sample for hand morphology and craniometric data for these 4 taxa.

Herein, we use separate multivariate analyses of the manus and the skull to assess the potential morphological distinctiveness of Javan *T. “glis” hypochrysa* (hereafter *T. hypochrysa*) from *T. glis*, with which it is currently synonymized; from Sumatran *T. ferruginea*, of which it was originally considered a subspecies; and from *T. chrysogaster*. We included *T. chrysogaster* in these analyses primarily because Lyon (1913:36) paired this taxon with *T. hypochrysa* to form his Hypochrysa Group, indicating that he thought they formed a natural grouping. Although we now know that the 2 taxa differ in mammae formula (Sargis et al. 2013: table 1), this does not nullify Lyon’s implicit hypothesis. The only other treeshrew known from Java is Horsfield’s treeshrew, *T. javanica* Horsfield, 1822 (Lyon 1913; Roberts et al. 2011). We did not include this species in our study because it is distantly related to the *T. glis* species complex (Olson et al. 2004b, 2005; Roberts et al. 2011), and these 2 taxa are distinct in body size (Endo et al. 2003) as well as skull (Endo et al. 2003, 2004) and postcranial skeletal (Sargis 2002a, 2002b, 2002c) morphology.

TABLE 1.—Measurements (mm) of bones in the manus of selected species of *Tupaia*. Statistics are mean \pm SD, range of measurements, and sample size in parentheses. Because of its orientation in the X-rays, depth was measured for ray I; width was measured for the other 4 rays (see “Materials and Methods”).

	Metacarpal length (ML)	Metacarpal depth/width (MD/MW)	Proximal phalanx length (PPL)	Proximal phalanx depth/width (PPD/PPW)	Middle phalanx length (MPL)	Middle phalanx width (MPW)	Distal phalanx length (DPL)	Distal phalanx depth/width (DPD/DPW)
Ray I								
<i>T. chrysogaster</i>	4.53 \pm 0.25 4.09–4.88 (12)	0.70 \pm 0.05 0.61–0.79 (12)	3.45 \pm 0.32 2.77–3.93 (12)	0.69 \pm 0.06 0.61–0.80 (12)			2.57 \pm 0.17 2.25–2.82 (11)	1.24 \pm 0.13 1.07–1.45 (12)
<i>T. glis</i>	4.21 \pm 0.28 3.59–5.13 (33)	0.59 \pm 0.07 0.49–0.84 (33)	3.33 \pm 0.17 2.90–3.76 (32)	0.62 \pm 0.07 0.50–0.79 (32)			2.36 \pm 0.27 1.47–2.94 (32)	1.05 \pm 0.12 0.87–1.27 (29)
<i>T. ferruginea</i>	4.59 \pm 0.29 3.91–4.96 (13)	0.62 \pm 0.06 0.52–0.72 (13)	3.57 \pm 0.13 3.30–3.74 (13)	0.64 \pm 0.05 0.52–0.72 (13)			2.45 \pm 0.20 1.98–2.73 (12)	1.19 \pm 0.16 0.96–1.41 (12)
<i>T. hypochrysa</i>	4.58 \pm 0.19 4.40–4.82 (4)	0.68 \pm 0.08 0.62–0.79 (4)	3.50 \pm 0.23 3.16–3.64 (4)	0.65 \pm 0.06 0.60–0.73 (4)			2.73 \pm 0.16 2.55–2.86 (3)	1.23 \pm 0.25 1.08–1.52 (3)
Ray II								
<i>T. chrysogaster</i>	8.34 \pm 0.61 7.33–9.39 (10)	0.83 \pm 0.08 0.66–0.91 (8)	4.89 \pm 0.22 4.61–5.35 (11)	0.76 \pm 0.05 0.67–0.85 (8)	2.82 \pm 0.15 2.61–3.01 (9)	0.79 \pm 0.04 0.75–0.86 (5)	2.62 \pm 0.34 1.85–3.16 (12)	1.11 \pm 0.05 1.06–1.18 (7)
<i>T. glis</i>	7.53 \pm 0.42 6.91–8.92 (31)	0.72 \pm 0.06 0.63–0.84 (28)	4.58 \pm 0.31 3.64–5.01 (34)	0.69 \pm 0.05 0.57–0.78 (26)	2.76 \pm 0.19 2.32–3.20 (29)	0.69 \pm 0.07 0.56–0.82 (18)	2.22 \pm 0.31 1.65–2.91 (31)	1.02 \pm 0.09 0.87–1.23 (14)
<i>T. ferruginea</i>	8.13 \pm 0.57 6.88–8.95 (13)	0.75 \pm 0.05 0.67–0.82 (10)	5.00 \pm 0.28 4.35–5.36 (13)	0.72 \pm 0.07 0.63–0.89 (11)	2.86 \pm 0.21 2.36–3.13 (11)	0.73 \pm 0.04 0.67–0.79 (9)	1.98 \pm 0.27 1.56–2.39 (12)	1.02 \pm 0.06 0.95–1.09 (8)
<i>T. hypochrysa</i>	8.24 \pm 0.62 7.54–8.72 (3)	0.86 \pm 0.05 0.81–0.92 (4)	4.99 \pm 0.27 4.70–5.24 (3)	0.73 \pm 0.03 0.71–0.76 (4)	3.02 (1)	0.78 \pm 0.08 0.67–0.84 (4)	2.47 \pm 0.12 2.34–2.60 (4)	1.13 \pm 0.15 0.96–1.23 (3)

TABLE 1.—Continued.

	Metacarpal length (ML)	Metacarpal depth/width (MD/MW)	Proximal phalanx length (PPL)	Proximal phalanx depth/width (PPD/PPW)	Middle phalanx length (MPL)	Middle phalanx width (MPW)	Distal phalanx length (DPL)	Distal phalanx depth/width (DPD/DPW)
Ray III								
<i>T. chrysogaster</i>	10.41 ± 0.63 9.55–11.70 (10)	0.82 ± 0.04 0.77–0.89 (10)	5.09 ± 0.17 4.79–5.36 (10)	0.78 ± 0.04 0.71–0.82 (7)	3.06 ± 0.17 2.82–3.37 (10)	0.72 ± 0.03 0.67–0.77 (7)	2.51 ± 0.30 2.27–3.04 (12)	1.12 ± 0.06 1.04–1.18 (5)
<i>T. glis</i>	9.39 ± 0.50 8.60–10.42 (29)	0.75 ± 0.05 0.68–0.86 (25)	4.77 ± 0.29 4.05–5.36 (33)	0.75 ± 0.06 0.65–0.88 (33)	3.00 ± 0.32 2.45–3.76 (29)	0.69 ± 0.06 0.59–0.81 (27)	2.16 ± 0.34 1.61–2.97 (30)	1.05 ± 0.10 0.88–1.23 (18)
<i>T. ferruginea</i>	10.32 ± 0.50 9.53–11.20 (12)	0.79 ± 0.06 0.68–0.89 (10)	5.19 ± 0.21 4.77–5.57 (13)	0.73 ± 0.04 0.66–0.78 (13)	3.31 ± 0.17 3.09–3.61 (10)	0.71 ± 0.05 0.66–0.83 (10)	2.03 ± 0.31 1.49–2.45 (11)	1.06 ± 0.07 0.90–1.14 (8)
<i>T. hypochrysa</i>	10.22 9.48–10.96 (2)	0.88 ± 0.03 0.85–0.91 (3)	5.35 ± 0.19 5.22–5.57 (3)	0.83 ± 0.04 0.78–0.85 (3)	3.03 (1)	0.79 ± 0.00 0.79–0.79 (3)	2.46 ± 0.41 1.87–2.78 (4)	1.19 1.17–1.21 (2)
Ray IV								
<i>T. chrysogaster</i>	9.51 ± 0.19 9.15–9.81 (8)	0.82 ± 0.06 0.68–0.88 (8)	4.99 ± 0.20 4.70–5.42 (12)	0.78 ± 0.06 0.71–0.89 (9)	3.12 ± 0.19 2.86–3.40 (9)	0.72 ± 0.05 0.66–0.79 (7)	2.60 ± 0.24 2.24–2.95 (12)	1.05 ± 0.10 0.94–1.13 (3)
<i>T. glis</i>	8.56 ± 0.47 7.61–9.57 (29)	0.77 ± 0.07 0.67–0.95 (25)	4.65 ± 0.25 4.09–5.08 (34)	0.72 ± 0.06 0.62–0.83 (32)	2.94 ± 0.33 2.00–3.63 (29)	0.66 ± 0.07 0.56–0.78 (21)	2.22 ± 0.28 1.72–2.89 (29)	0.98 ± 0.09 0.88–1.23 (14)
<i>T. ferruginea</i>	9.08 ± 0.55 8.06–9.80 (8)	0.78 ± 0.05 0.71–0.87 (7)	5.08 ± 0.24 4.67–5.47 (13)	0.74 ± 0.06 0.66–0.86 (12)	3.34 ± 0.22 3.00–3.88 (12)	0.72 ± 0.07 0.56–0.82 (10)	2.13 ± 0.33 1.57–2.82 (11)	0.97 ± 0.05 0.90–1.05 (6)
<i>T. hypochrysa</i>	9.94 9.92–9.96 (2)	0.90 ± 0.03 0.88–0.94 (3)	5.21 ± 0.22 5.02–5.45 (3)	0.82 ± 0.03 0.80–0.85 (3)	3.62 (1)	0.78 0.72–0.83 (2)	2.64 ± 0.10 2.57–2.76 (3)	1.13 1.10–1.16 (2)
Ray V								
<i>T. chrysogaster</i>	5.90 ± 0.33 5.36–6.28 (9)	0.85 ± 0.09 0.72–1.00 (7)	4.07 ± 0.14 3.77–4.24 (12)	0.71 ± 0.06 0.63–0.81 (11)	2.27 (1)	0.79 ± 0.05 0.71–0.84 (4)	2.14 ± 0.29 1.63–2.58 (11)	1.00 ± 0.05 0.94–1.05 (4)
<i>T. glis</i>	5.51 ± 0.34 4.98–6.24 (31)	0.70 ± 0.08 0.55–0.80 (29)	3.89 ± 0.17 3.49–4.23 (34)	0.67 ± 0.05 0.55–0.79 (29)	2.17 ± 0.19 1.75–2.50 (18)	0.66 ± 0.07 0.54–0.77 (17)	1.90 ± 0.23 1.39–2.35 (30)	0.97 ± 0.09 0.81–1.18 (15)
<i>T. ferruginea</i>	5.83 ± 0.37 5.10–6.36 (12)	0.75 ± 0.08 0.60–0.85 (10)	4.10 ± 0.25 3.80–4.56 (13)	0.70 ± 0.05 0.64–0.80 (11)	2.30 ± 0.17 2.06–2.53 (10)	0.68 ± 0.04 0.62–0.75 (8)	1.98 ± 0.20 1.62–2.32 (13)	0.97 ± 0.10 0.84–1.15 (7)
<i>T. hypochrysa</i>	6.32 ± 0.44 5.67–6.65 (4)	0.82 ± 0.03 0.77–0.84 (4)	4.02 3.91–4.13 (2)	0.75 ± 0.05 0.67–0.78 (4)	– (0)	0.73 0.69–0.76 (2)	2.27 ± 0.20 2.07–2.46 (4)	1.08 (1)

MATERIALS AND METHODS

Manus.—For analyses of the hands, we used measurements previously obtained from digital X-ray images of dried study skins of 64 specimens of *T. chrysogaster* ($n = 12$), *T. ferruginea* ($n = 13$), *T. glis* ($n = 35$), and *T. hypochrysa* ($n = 4$). These specimens were included in previous analyses by Sargis et al. (2013), but here we include 2 additional specimens of *T. hypochrysa*, including the holotype, from The Natural History Museum (BMNH) and 1 from the American Museum of Natural History (AMNH; see Appendix I). Forefeet of the AMNH specimen were X-rayed using a Kevex-Varian (Palo Alto, California) digital X-ray system in the United States National Museum of Natural History (USNM) following the procedure of Sargis et al. (2013). The 2 BMNH specimens were X-rayed at the BMNH in London. The resulting digital images were transferred to Adobe Photoshop CS4 Extended

(2008), trimmed, converted to positive images, and measured by NCM with the custom Measurement Scale in the Analysis menu. Measurements were taken from either the right or left side, and supplemented, where necessary and possible, by measurements from the image of the other side. We recorded the following measurements from all 5 rays (38 total), with the exception that depths (dorsopalmar distances) of bones were substituted for widths (mediolateral distances) in ray I because of its orientation in the images: DPD = distal phalanx depth; DPL = distal phalanx length; DPW = distal phalanx width; MD = metacarpal depth; ML = metacarpal length; MW = metacarpal width; MPL = middle phalanx length; MPW = middle phalanx width; PPD = proximal phalanx depth; PPL = proximal phalanx length; PPW = proximal phalanx width (see Sargis et al. 2013: fig. 1). A numeral before an abbreviation designates the ray (e.g., 4MW = width of metacarpal IV). All

TABLE 2.—Component loadings from principal components analyses (PCA) of manus proportions among individuals. Abbreviations for variables are defined in the “Materials and Methods.” Loadings in boldface type are discussed in the text.

	Axis		
	1	2	3
A) PCA of 6 variables from rays III and IV (Fig. 2A)			
3PPL	0.795	-0.512	0.224
4PPL	0.784	-0.526	0.245
4PPW	0.774	0.025	-0.486
3PPW	0.771	0.327	-0.362
3DPL	0.377	0.742	0.122
4DPL	0.476	0.565	0.502
Eigenvalues	2.809	1.516	0.744
Percentage of total variance explained	46.822	25.273	12.407
B) PCA of 8 variables from rays II, III, and V (Fig. 2B)			
2MW	0.795	0.220	0.427
5ML	0.770	0.290	0.381
3DPL	0.770	-0.406	0.142
5DPL	0.738	-0.190	-0.023
2PPW	0.699	0.103	-0.408
2DPL	0.692	-0.577	0.006
5PPW	0.675	0.063	-0.523
5MW	0.647	0.525	-0.140
Eigenvalues	4.205	0.957	0.808
Percentage of total variance explained	52.557	11.965	10.094

measurements are in millimeters and rounded to the nearest 0.01 mm. Summary statistics include mean, standard deviation, and total range (Table 1).

We carried out principal components analyses (PCA) on combinations of variables from individuals of the 4 taxa to determine how they vary in manus proportions. Because the focus of this study was the status of *T. hypochrysa*, we attempted to maximize its representation in all analyses. This yielded 2 models: a 6-variable model from rays III and IV

TABLE 3.—Mean factor scores and component loadings from principal components analysis of means of 6 variables from ray IV (Fig. 2C). Abbreviations for variables are defined in the “Materials and Methods.” Loadings in boldface type are discussed in the text.

	Axis	
	1	2
Mean factor scores		
<i>Tupaia chrysogaster</i>	0.216143	0.97791
<i>T. ferruginea</i>	-0.23253	-1.36747
<i>T. glis</i>	-1.19577	0.415944
<i>T. hypochrysa</i>	1.212163	-0.02638
Component loadings		
4MPW	0.995	-0.083
4ML	0.990	0.108
4PPW	0.968	0.220
4PPL	0.913	-0.373
4MPL	0.878	-0.438
4DPL	0.783	0.622
Eigenvalues	5.126	0.784
Percentage of total variance explained	85.427	13.060

TABLE 4.—Measurement descriptions (and abbreviations) following Sargis et al. (in press). The 9 measurements included in the PCA of individuals are indicated with an asterisk (see Table 6). Uppercase abbreviations for teeth (i.e., I, C, P, M) refer to maxillary and premaxillary teeth; lowercase abbreviations (i, c, p, m) refer to mandibular teeth.

- 1) Condylpremaxillary length (CPL): greatest distance between rostral surface of premaxilla and caudal surface of occipital condyle.
- 2) Condylincisive length (CIL): greatest distance between anterior-most surface of I1 and caudal surface of occipital condyle.
- 3) Upper tooth-row length (UTL): greatest distance between anterior-most surface of I1 and posterior-most surface of M3.*
- 4) Maxillary tooth-row length (MTL): greatest distance between anterior-most surface of C1 and posterior-most surface of M3.*
- 5) Epipterygoid-premaxillary length (EPL): greatest distance between rostral surface of premaxilla and caudal surface of epipterygoid process.
- 6) Palatopremaxillary length (PPL): greatest distance between rostral surface of premaxilla and caudal surface of palatine.*
- 7) Epipterygoid breadth (EB): greatest distance between lateral points of epipterygoid processes.
- 8) Mastoid breadth (MB): greatest distance between lateral apices of mastoid portion of petrosal.
- 9) Lacrimal breadth (LB): greatest distance between lateral apices of lacrimal tubercles.
- 10) Least interorbital breadth (LIB): least distance between the orbits.*
- 11) Zygomatic breadth (ZB): greatest distance between lateral surfaces of zygomatic arch.
- 12) Braincase breadth (BB): greatest breadth of braincase.
- 13) Lambdoid-premaxillary length (LPL): greatest distance between rostral surface of premaxilla and caudal surface of lambdoid crest.
- 14) Condylonasal length (CNL): greatest distance between rostral surface of nasal and caudal surface of occipital condyle.
- 15) Postorbital bar-premaxillary length (PBPL): greatest distance between rostral surface of premaxilla and caudal surface of postorbital bar.*
- 16) Lacrimal tubercle-premaxillary length (LTPL): greatest distance between rostral surface of premaxilla and caudal surface of lacrimal tubercle.*
- 17) Lambdoid crest height (LCH): greatest distance from apex (or apices if bilobate) of lambdoid crest to both ventral apices of occipital condyles (i.e., along midline).
- 18) Mandibular height (MH): greatest distance between coronoid and angular processes of mandible.*
- 19) Mandibular condyle height (MCH): greatest distance between mandibular condyle and angular process of mandible.*
- 20) Mandibular condyle width (MCW): greatest distance between medial and lateral surfaces of mandibular condyle.*
- 21) Mandibular condylincisive length (MCIL): greatest distance between anterior-most surface of i1 and caudal surface of mandibular condyle.
- 22) Lower tooth-row length (LTL): greatest distance between anterior-most surface of i1 and posterior-most surface of m3.

(3PPL, 3PPW, 3DPL, 4PPL, 4PPW, 4DPL) with 3 *T. hypochrysa*, and an 8-variable model from rays II, III, and V (2MW, 2PPW, 2DPL, 3DPL, 5ML, 5DPL, 5PPW, 5MW) that included all 4 specimens of *T. hypochrysa* (Table 2). We also used PCA to assess the separation of taxon means. This has the advantage of maximizing the number of variables available by permitting use of variables that are missing from individual specimens. Following Sargis et al. (2013), we used the same 6 variables from ray IV (4MPW, 4ML, 4PPW, 4PPL, 4MPL, 4DPL; Table 3) in our analysis of taxon means.

To determine the overall similarity of the manus among all 4 taxa, we performed a hierarchical cluster analysis on 37 available variables (5MPL lacking) from all 5 rays. The

TABLE 5.—Craniodental measurements (mm) of selected species of *Tupaia*. Statistics are mean \pm SD, range of measurements, and sample size in parentheses. See Table 4 for measurement abbreviations and descriptions.

	1) CPL	2) CIL	3) UTL	4) MTL	5) EPL	6) PPL	7) EB	8) MB	9) LB	10) LIB	11) ZB
<i>Tupaia chrysogaster</i>	50.12 \pm 1.30 47.99–52.66 (19)	49.36 \pm 1.20 47.20–51.60 (18)	28.59 \pm 0.75 27.27–29.99 (20)	19.79 \pm 0.56 18.90–20.91 (22)	37.13 \pm 1.14 34.81–38.78 (12)	30.54 \pm 0.91 29.11–32.58 (21)	12.26 \pm 0.77 11.51–13.56 (9)	18.57 \pm 0.41 17.51–19.23 (21)	19.35 \pm 0.58 18.66–21.08 (18)	14.53 \pm 0.51 13.51–15.57 (21)	26.77 \pm 0.55 25.36–27.95 (20)
<i>Tupaia glis</i>	46.57 \pm 1.51 43.26–49.96 (30)	45.90 \pm 1.55 42.85–49.23 (29)	26.24 \pm 1.05 23.90–29.21 (27)	18.06 \pm 0.68 16.70–20.22 (30)	33.99 \pm 1.52 30.48–36.96 (20)	27.80 \pm 0.92 25.27–29.47 (27)	11.54 \pm 0.63 10.48–12.55 (16)	17.77 \pm 0.44 16.99–18.51 (31)	18.32 \pm 0.86 16.26–19.88 (22)	14.21 \pm 0.67 13.03–15.79 (34)	24.91 \pm 0.84 23.26–26.62 (31)
<i>Tupaia ferruginea</i>	48.59 \pm 1.01 46.84–50.93 (47)	47.92 \pm 0.99 46.22–50.38 (47)	27.32 \pm 0.62 25.65–29.03 (59)	19.03 \pm 0.43 18.23–19.93 (60)	35.21 \pm 0.98 33.14–37.19 (40)	29.00 \pm 0.71 27.70–30.83 (51)	11.94 \pm 0.65 9.77–12.71 (22)	18.17 \pm 0.51 17.32–19.42 (47)	18.71 \pm 0.62 17.16–20.00 (47)	14.63 \pm 0.63 11.99–15.70 (59)	25.56 \pm 0.92 21.55–27.14 (49)
<i>Tupaia hypochrysa</i>	49.44 \pm 2.52 45.84–51.49 (4)	48.78 \pm 2.47 45.22–50.88 (4)	28.44 \pm 1.32 25.77–29.82 (7)	19.64 \pm 0.65 18.45–20.66 (8)	37.98 \pm 0.28 37.78–38.18 (2)	30.54 \pm 1.44 27.34–31.86 (8)	12.11 (1)	18.76 \pm 0.50 18.21–19.20 (3)	19.40 \pm 0.88 18.49–20.24 (3)	14.76 \pm 0.66 13.19–15.26 (8)	26.48 \pm 0.69 25.79–27.63 (5)

TABLE 5.—Continued.

	12) BB	13) LPL	14) CNL	15) PBPL	16) LTP	17) LCH	18) MH	19) MCH	20) MCW	21) MCIL	22) LTL
<i>Tupaia chrysogaster</i>	19.80 \pm 0.39 19.07–20.34 (20)	54.43 \pm 1.35 52.20–57.50 (19)	49.20 \pm 1.18 47.09–51.45 (19)	37.50 \pm 0.99 35.20–39.15 (20)	26.06 \pm 0.93 23.91–27.82 (21)	13.28 \pm 0.37 12.63–14.28 (21)	14.58 \pm 0.68 13.38–16.12 (24)	9.57 \pm 0.44 8.64–10.63 (24)	3.67 \pm 0.18 3.34–4.01 (24)	40.62 \pm 1.07 38.51–43.72 (20)	27.28 \pm 0.76 26.36–29.40 (19)
<i>Tupaia glis</i>	18.98 \pm 0.40 17.87–19.64 (32)	49.91 \pm 1.70 46.10–53.72 (29)	44.68 \pm 1.60 41.53–49.07 (30)	33.94 \pm 1.41 29.87–36.77 (31)	23.29 \pm 1.31 19.94–26.45 (30)	12.19 \pm 0.42 11.42–13.22 (32)	13.46 \pm 0.66 11.88–14.80 (34)	8.87 \pm 0.47 7.82–10.06 (34)	3.14 \pm 0.22 2.81–3.53 (34)	36.92 \pm 1.31 33.71–40.76 (32)	24.83 \pm 0.90 22.73–27.46 (31)
<i>Tupaia ferruginea</i>	19.66 \pm 0.52 17.93–20.61 (48)	51.79 \pm 1.62 44.29–54.15 (43)	46.99 \pm 1.02 44.67–49.08 (41)	34.91 \pm 1.33 27.62–37.71 (57)	23.92 \pm 1.05 18.30–26.40 (59)	12.43 \pm 0.31 11.69–13.03 (46)	13.98 \pm 0.67 11.82–15.34 (61)	9.31 \pm 0.47 8.23–10.25 (62)	3.17 \pm 0.25 2.52–3.69 (62)	38.32 \pm 0.82 36.60–40.54 (60)	25.69 \pm 0.90 20.14–27.00 (58)
<i>Tupaia hypochrysa</i>	19.88 \pm 0.63 19.04–20.57 (4)	52.29 \pm 1.80 50.21–53.36 (3)	48.30 \pm 3.16 43.89–50.93 (4)	36.79 \pm 1.55 33.33–38.03 (8)	25.25 \pm 1.29 22.86–26.49 (7)	12.68 \pm 0.85 12.08–13.28 (2)	14.91 \pm 0.63 13.96–16.04 (7)	10.02 \pm 0.47 9.44–10.63 (7)	3.76 \pm 0.14 3.57–4.01 (8)	39.80 \pm 1.78 36.67–41.03 (5)	26.99 \pm 1.32 24.65–28.58 (6)

TABLE 6.—Component loadings from principal components analysis of skulls using individuals (Fig. 3A). Abbreviations for variables are defined in Table 4. Loadings in boldface type are discussed in the text.

	Axis		
	1	2	3
3) UTL	0.943	−0.231	−0.114
4) MTL	0.904	−0.196	−0.040
6) PPL	0.965	−0.180	−0.045
10) LIB	0.644	−0.141	0.709
15) PBPL	0.960	−0.183	−0.078
16) LTPL	0.952	−0.172	−0.069
18) MH	0.797	0.508	0.047
19) MCH	0.758	0.572	0.145
20) MCW	0.764	0.209	− 0.360
Eigenvalues	6.674	0.836	0.683
Percentage of total variance explained	74.157	9.285	7.591

phenogram from this analysis is presented with Euclidean distances.

Skull.—For our analyses of the cranium and mandible, we recorded the same 22 measurements (Table 4) used by Sargis et al. (in press) in their study of treeshrews from the Palawan faunal region. These measurements were taken to the nearest 0.01 mm using digital calipers. Our craniodental sample included the same specimens of *T. glis* ($n = 35$) from the manus analyses, and larger samples of *T. chrysogaster* ($n = 25$), *T. ferruginea* ($n = 64$), and *T. hypochrysa* ($n = 8$), including the holotypes of the latter 3 taxa. A total of 132 adult (those with fully erupted permanent dentition) skulls was included in this portion of the study (see Appendix I). Summary craniodental statistics are presented in Table 5.

The PCA of skull variables for individuals included 9 variables (Table 6), whereas the PCA of taxon means included all 22 (Table 7); the elimination of 13 variables in the PCA of individuals allowed the inclusion of several specimens, particularly from *T. hypochrysa*, that were missing data due to breakage. The PCA of individuals and means include different numbers of variables (9 versus 22, respectively), so they yield different results in morphospace (Sargis et al. 2013). We also conducted cluster analyses (unweighted pair-group average) of taxon means, which included all 22 skull variables and a combination of the 22 skull variables and 37 manus variables for a total of 59.

RESULTS

Manus.—Our morphometric analyses of the potential distinctiveness of the manus yielded 2 models that included 3–4 individuals of *T. hypochrysa*. In our analysis of 6 variables from rays III and IV (3PPL, 3PPW, 3DPL, 4PPL, 4PPW, 4DPL), the 1st factor axis is a size axis dominated by the lengths and widths of the proximal phalanges from the 2 rays, representing almost 47% of the total variation (Table 2A). The 2nd axis, which accounts for more than 25% of the variation, is a contrast between the lengths of the distal phalanges and the

TABLE 7.—Mean factor scores and component loadings from principal components analysis of means of 22 skull variables (Fig. 3B). Abbreviations for variables are defined in Table 4.

	Axis		
	1	2	3
Mean factor scores			
<i>Tupaia chrysogaster</i>	3.873	−1.359	0.007
<i>Tupaia ferruginea</i>	−1.351	0.454	1.121
<i>Tupaia glis</i>	−5.756	−0.328	−0.572
<i>Tupaia hypochrysa</i>	3.234	1.234	−0.557
Component loadings			
1) CPL	0.979	−0.074	0.187
2) CIL	0.980	−0.046	0.191
3) UTL	1.000	0.003	0.000
4) MTL	0.993	0.018	0.117
5) EPL	0.960	0.201	−0.193
6) PPL	0.998	0.043	−0.050
7) EB	0.980	−0.091	0.179
8) MB	0.972	0.217	−0.089
9) LB	0.990	0.061	−0.130
10) LIB	0.776	0.558	0.295
11) ZB	0.992	−0.105	−0.063
12) BB	0.935	0.226	0.274
13) LPL	0.906	−0.381	0.185
14) CNL	0.987	−0.097	0.131
15) PBPL	0.979	−0.162	−0.121
16) LTPL	0.960	−0.253	−0.121
17) LCH	0.870	−0.493	−0.001
18) MH	0.963	0.231	−0.141
19) MCH	0.900	0.417	−0.126
20) MCW	0.915	0.040	−0.401
21) MCIL	0.988	−0.153	−0.002
22) LTL	0.994	−0.072	−0.081
Eigenvalues	20.141	1.228	0.632
Percentage of total variance explained	91.548	5.581	2.871

lengths of the proximal phalanges of both rays. In the plot of factor scores on these 2 axes (Fig. 2A), *T. hypochrysa* plots high on the 1st axis as a result of its longer, broader proximal phalanges. Individuals of *T. chrysogaster* average the next largest, whereas *T. ferruginea* and *T. glis* are broadly dispersed and overlap the range of *T. chrysogaster*, but *T. glis* is typically smaller. Along the 2nd factor axis, most specimens of *T. ferruginea* plot low because of their shorter distal phalanges, particularly in relation to their proximal phalanges.

Our analysis using 8 variables from rays II, III, and V (2MW, 2PPW, 2DPL, 3DPL, 5ML, 5DPL, 5PPW, 5MW) included all 4 specimens of *T. hypochrysa*. Here, the 1st factor axis, which accounts for more than 52% of the variation, is a size variable with relatively high loadings for all 8 variables (Table 2B). Factor 2, representing nearly 12% of the variation, is a contrast between the width of metacarpal V (5MW) and the length of distal phalanx II (2DPL). A plot of factor scores on these 2 axes (Fig. 2B) shows *T. hypochrysa* and *T. chrysogaster* plotting high on the 1st factor axis, indicating their typically larger size compared with the other 2 species. Although there is considerable overlap, *T. glis* typically has the smallest rays among these species, and *T. ferruginea* is

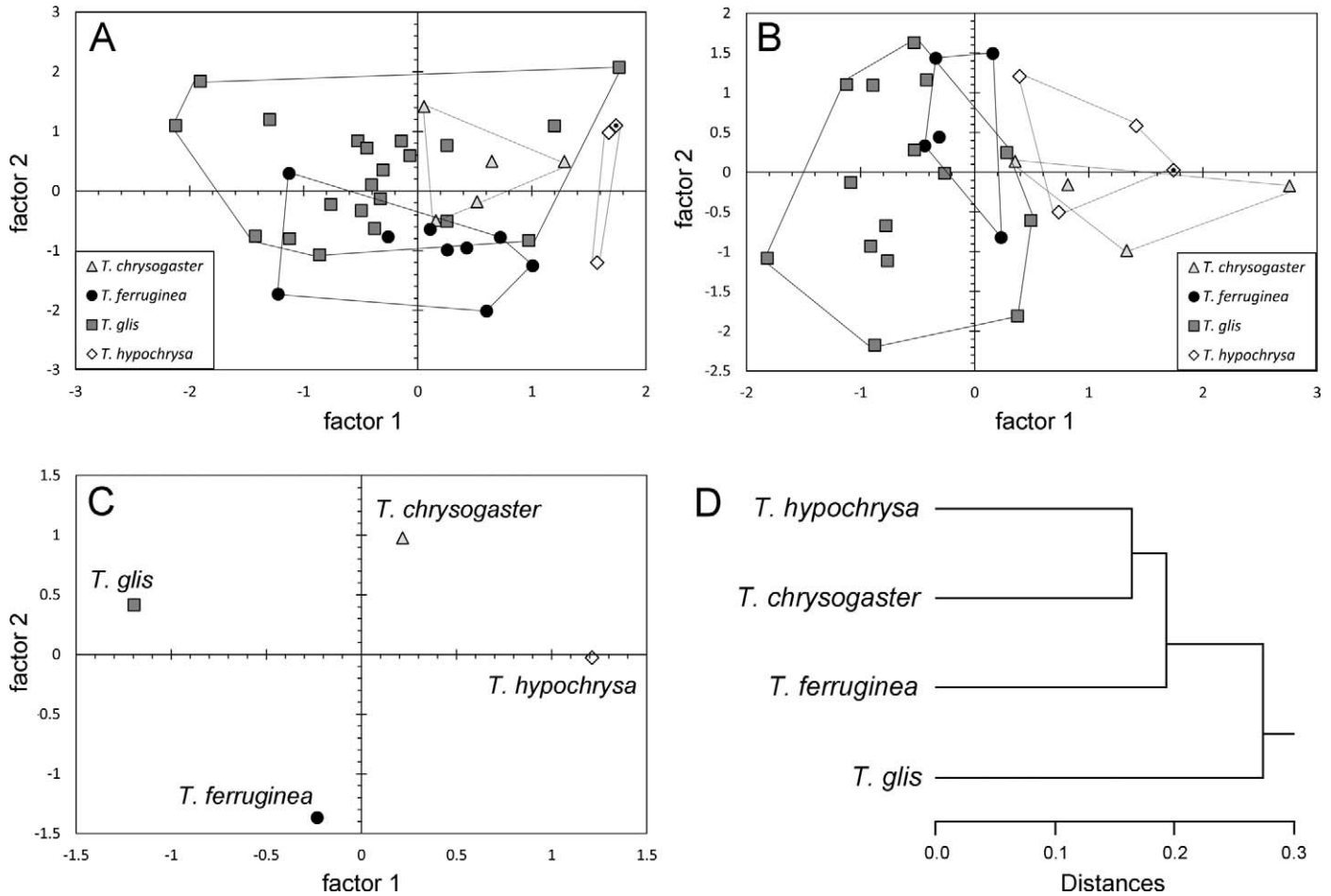


FIG. 2.—Plots of factor scores from principal components analyses (PCA) illustrating the distinctiveness of the manus of *T. hypochrysa*. The holotype of *T. hypochrysa* is marked by a solid black dot within the diamond symbol for that taxon. A) Plot of factor scores on the first 2 factor axes from PCA of 6 variables from rays III and IV (Table 2A). B) Plot of factor scores on the first 2 factor axes from PCA of 8 variables from rays II, III, and V (Table 2B). C) Plot of factor scores on the first 2 factor axes from PCA of the means of 6 variables from ray IV (Table 3). D) Phenogram from cluster analysis of 37 variables from all 5 rays. *T. hypochrysa* is more similar to *T. chrysogaster* than to *T. glis*.

intermediate in size. Along the 2nd factor axis, *T. hypochrysa* and *T. chrysogaster* show a tendency to separate (with some overlap), a result of the typically broader metacarpal V and shorter distal phalanx II of *T. hypochrysa*. *T. ferruginea* is generally higher on this axis, whereas *T. glis* exhibits a greater range of variation than that shown by the remaining 3 species combined. The 2 analyses of individuals show incomplete separation among many of the groups, although *T. hypochrysa* is consistently the most distinctive of the 4 taxa, and it averages the largest lengths or widths for many of the individual bones.

The PCA of means of 6 variables from ray IV yielded a model in which the 1st factor axis, representing more than 85% of the variation, is a size axis (Table 3). The plot of factor scores (Fig. 2C) confirms a general pattern of increasing overall size of the manus from the smallest in *T. glis*, to intermediate-sized *T. ferruginea* and *T. chrysogaster*, to largest in *T. hypochrysa*. The 2nd factor axis, accounting for 13% of the variation, is a contrast between the lengths of the distal and middle phalanges. Along this axis, *T. chrysogaster* has the longest distal phalanx (and potentially the longest claw), with

T. glis and *T. hypochrysa* intermediate in size, and *T. ferruginea* having the shortest distal phalanx.

Cluster analysis of 37 variables from all 5 rays shows a hierarchical clustering, with *T. chrysogaster* and *T. hypochrysa* most similar to one another and *T. ferruginea* most similar to that grouping (Fig. 2D). *T. glis* is the least similar to the other 3 taxa.

Skull.—The PCA of individuals included 9 of the 22 craniodental variables. Factor 1 is a size vector that accounts for more than 74% of the variation. The 2nd factor represents mandibular height (MH) and mandibular condyle height (MCH), and is responsible for more than 9% of the variation (Table 6). Factor 3 represents least interorbital breadth (LIB) contrasted with mandibular condyle width (MCW) and explains more than 7.5% of the variation (Table 6). In a plot of factors 1 and 2 (not shown), there is no overlap between *T. hypochrysa* and *T. glis*. Better resolution, however, is shown in the plot of the 1st and 3rd factors (Fig. 3A); *T. hypochrysa* overlaps with *T. chrysogaster* rather than *T. glis*, mostly in positive morphospace along factor 1, and *T. glis* overlaps with

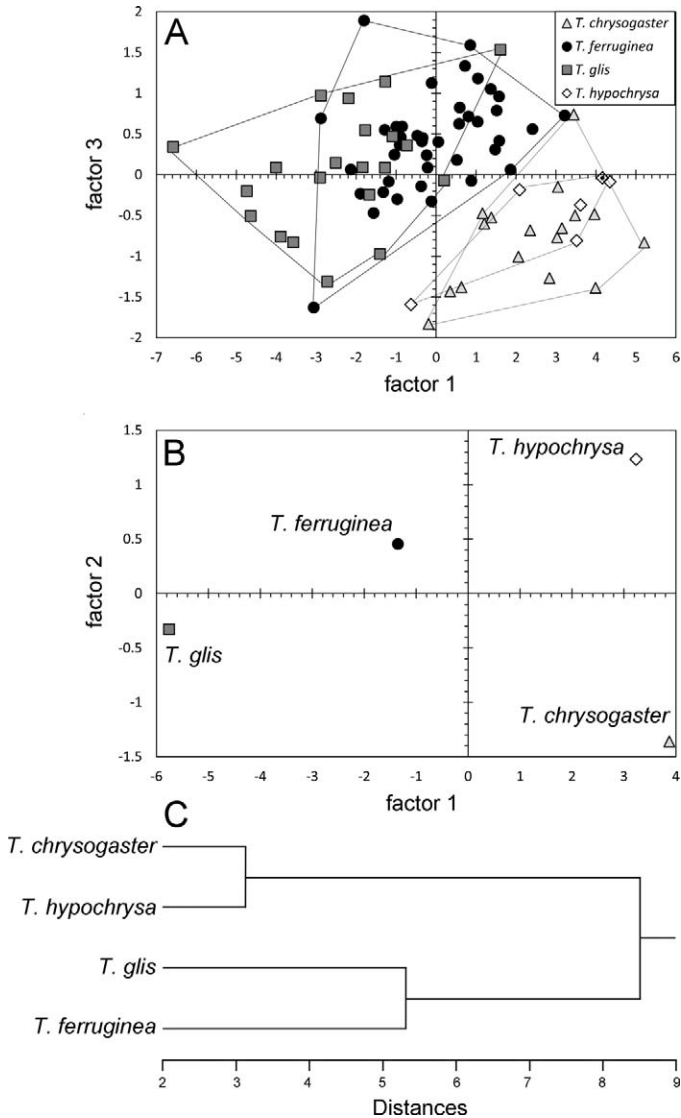


FIG. 3.—Plots of factor scores from principal components analyses (PCA) illustrating results of craniodental analyses. The holotype of *T. hypochrysa* is marked by a solid black dot within the diamond symbol for that taxon. A) Plot of individual factor scores on the 1st and 3rd axes from PCA of 9 variables (Table 6). In this plot, there is clear separation between *T. hypochrysa*–*T. chrysogaster* and *T. ferruginea*–*T. glis*. B) Plot of factor scores on the first 2 axes from PCA of the means of all 22 variables (Table 7). C) Phenogram from cluster analysis of all 22 variables. *T. hypochrysa* is more similar to *T. chrysogaster* than to *T. glis*.

T. ferruginea, mostly in negative morphospace along the 1st factor.

For the PCA of taxon means, all 22 craniodental variables were included in the analysis. Factor 1 is again a size vector and represents more than 91% of the variation, and factor 2 accounts for more than 5.5% (Table 7). The 4 taxa plot in different quadrants (Fig. 3B), with *T. hypochrysa* and *T. chrysogaster* in positive morphospace along factor 1 and *T. glis* and *T. ferruginea* in negative morphospace along that factor. *T. hypochrysa* plots in positive morphospace along factor 2 as

well, whereas *T. glis* is in negative morphospace for the 2nd factor.

We carried out cluster analyses of taxon means on the 22 craniodental variables and 59 variables combined from the skull and manus. The 2 analyses yielded the same topology, so only the results from the analysis of skull variables are shown in Fig. 3. In both analyses, *T. hypochrysa* is most similar to *T. chrysogaster*, rather than *T. glis*, whereas the latter is most similar to *T. ferruginea* (Fig. 3C).

DISCUSSION

The results of our analyses of hand and skull morphology are congruent in demonstrating the distinctiveness of Javan *T. hypochrysa* relative to *T. glis*. In fact, the Javan taxon is far more similar in both manual and cranial morphology to *T. chrysogaster* from the Mentawai Islands than it is to either *T. ferruginea* from Sumatra or *T. glis* (Figs. 2 and 3). The former 2 taxa also share the loss of the entepicondylar foramen of the humerus, whereas the latter 2 species retain it (Sargis 2002a; Sargis et al. 2013: table 1). Therefore, *T. hypochrysa* is certainly morphologically and, we suggest, taxonomically distinct from *T. glis*. *T. hypochrysa* and *T. chrysogaster* can be distinguished by their different mammae counts, with 4 in the Javan taxon and 2 in the species from the Mentawai Islands (Sargis et al. 2013: table 1).

Our recognition of *T. hypochrysa* from Java as a distinct species is in agreement with Lyon's (1913) classification. Furthermore, the morphometric similarity between *T. hypochrysa* and *T. chrysogaster* (Figs. 2B and 3A) supports Lyon's Hypochrysa Group and may suggest a close relationship between the two. Taxonomic recognition of Javan *T. hypochrysa* and the phenetic support for Lyon's (1913) hypothesis regarding its affinities with *T. chrysogaster* underscore the need for additional molecular analyses to firmly establish the phylogenetic relationships among these and other closely related species.

Recognition of *T. hypochrysa* as distinct from the more widely distributed *T. glis* necessitates a re-evaluation of the conservation status of populations throughout Java, especially given its reported scarcity on that island: “[t]his species is very rare on Java, with only a single specimen in the last 100 years” (Boeadi pers. comm. in Han 2008). Furthermore, treeshrews inhabit tropical forests, and Java has less than 10% of its natural forest cover left (Lavigne and Gunnell 2006). Given these factors, it is possible that *T. hypochrysa* is vulnerable to extinction.

Our taxonomic revision has conservation implications for *T. glis* as well. The separation of Javan *T. hypochrysa* from *T. glis* further restricts the geographic distribution of the latter species to the Malay Peninsula south of the Isthmus of Kra (~10° N latitude) and the small neighboring islands (Fig. 1). The formerly widespread *T. glis* is listed as a species of “Least Concern” (Han 2008) on the *IUCN Red List of Threatened Species* (IUCN 2012), but its status requires reassessment considering the removal of the islands of Java, Sumatra, and

Bangka from its known geographic range (Sargis et al. 2013; Fig. 1).

Both *T. glis* and *T. hypochrysa*, as well as 3 recently resurrected taxa from Indonesia—*T. discolor* (Bangka Island), *T. ferruginea* (Sumatra), and *T. salatana* (southern Borneo)—are distributed in Sundaland, which has been characterized as one of the world's hottest biodiversity hotspots (Myers et al. 2000), and each of these species may represent relatively small, potentially vulnerable populations. Most occur on islands and, as is definitely the case with *T. glis*, may be far less widespread than previously thought. Our ongoing study of the *T. glis* species complex throughout Sundaland exemplifies the critical need for continued research on species limits in problematic and cryptic taxa (Olson et al. 2004a; Schlick-Steiner et al. 2007) in this geologically complex and threatened region.

ACKNOWLEDGMENTS

This research was supported by National Science Foundation grant DEB-0542532/0542725 and an Alaska EPSCoR grant to EJS and LEO. Additional support was provided to NW from the United States Geological Survey's Patuxent Wildlife Research Center and to NCM from the Yale Peabody Museum of Natural History Summer Internship Program. We thank the following curators, collection managers, and museums for access to the specimens in their collections: E. Westwig, D. Lunde, and R. Voss, AMNH, New York; R. Portela-Miguez, L. Tomsett, and P. Jenkins, BMNH, London; B. Stanley and L. Heaney, Field Museum of Natural History (FMNH), Chicago; J. Dines, Los Angeles County Museum of Natural History, Los Angeles (LACM); J. Chupasko and M. Omura, Museum of Comparative Zoology at Harvard University (MCZ), Cambridge, Massachusetts; C. Conroy and J. Patton, Museum of Vertebrate Zoology at University of California, Berkeley (MVZ); R. Winkler, Naturhistorisches Museum Basel (NMB); B. Herzig, A. Bibl, A. Gamauf, Naturhistorisches Museum Wien, Vienna (NMW); H. van Grouw, Nationaal Natuurhistorisch Museum, Leiden (RMNH); L. Gordon, R. Thorington, K. Helgen, and D. Lunde, USNM, Washington, DC; R. Angermann and F. Mayer, Museum für Naturkunde (ZMB), Berlin; and M. Anderson, Zoologisk Museum University of Copenhagen (ZMUC). We are grateful to S. Raredon, Division of Fishes, Museum Support Center, USNM, for assistance with the digital X-ray system, and to R. Portela-Miguez, Department of Zoology, BMNH, for providing X-rays of the 2 BMNH *T. hypochrysa* specimens. We thank E. Meijaard and an anonymous reviewer for comments that improved the manuscript. Any use of trade, product, or firm names is for descriptive purposes only and does not imply endorsement by the United States government.

LITERATURE CITED

- ADOBE PHOTOSHOP CS4 EXTENDED. 2008. Version 11.0.2, Adobe Systems Inc., San Jose, California.
- CARLSSON, A. 1922. Über die Tupaiidae und ihre Beziehungen zu den Insectivora und den Prosimiae. *Acta Zoologica*, Stockholm 3:227–270.
- CHASEN, F. N. 1940. A handlist of Malaysian mammals. *Bulletin of the Raffles Museum*, Singapore 15:1–209.
- DIARD, P. M. 1820. Report of a meeting of the Asiatic Society for March 10. *Asiatic Journal and Monthly Register* 10:477–478.
- ENDO, H., T. HIKIDA, L. M. CHOU, K. FUKUTA, AND B. J. STAFFORD. 2004. Proportion and cluster analyses of the skull in various species of the tree shrews. *Journal of Veterinary Medical Science* 66:1–7.
- ENDO, H., T. HIKIDA, M. MOTOKAWA, L. M. CHOU, K. FUKUTA, AND B. J. STAFFORD. 2003. Morphological adaptation of the skull for various behaviors in the tree shrews. *Journal of Veterinary Medical Science* 65:873–879.
- HAN, K.-H. 2008. *Tupaia glis*. In IUCN 2012. IUCN Red List of threatened species. Version 2012.2. www.iucnredlist.org. Accessed 19 January 2013.
- HELGEN, K. M. 2005. Order Scandentia. Pp. 104–109 in *Mammal species of the world: a taxonomic and geographic reference*. 3rd ed. (D. E. Wilson and D. M. Reeder, eds.). Johns Hopkins University Press, Baltimore, Maryland.
- HONACKI, J. H., K. E. KINMAN, AND J. W. KOEPL. 1982. *Mammal species of the world: a taxonomic and geographic reference*. 1st ed. Allen Press, Inc., Lawrence, Kansas.
- HORSFIELD, T. 1822. *Zoological researches in Java and the neighboring islands*. Kingbury, Parbury, and Allen, London.
- IUCN. 2012. The IUCN Red List of threatened species. Version 2012.2. www.iucnredlist.org. Accessed 19 January 2013.
- LAVIGNE, F., AND Y. GUNNELL. 2006. Land cover change and abrupt environmental impacts on Javan volcanoes, Indonesia: a long-term perspective on recent events. *Regional Environmental Change* 6:86–100.
- LYON, M. W. 1913. Treeshrews: an account of the mammalian family Tupaiidae. *Proceedings of the United States National Museum* 45:1–188.
- MILLER, G. S. 1903. Seventy new Malayan mammals. *Smithsonian Miscellaneous Collections* 45:1–73.
- MYERS, N., R. A. MITTERMEIER, C. G. MITTERMEIER, G. A. B. DA FONSECA, AND J. KENT. 2000. Biodiversity hotspots for conservation priorities. *Nature* 403:853–858.
- NAPIER, J. R., AND P. H. NAPIER. 1967. *A handbook of living primates*. Academic Press, New York.
- OLSON, L. E., S. M. GOODMAN, AND A. D. YODER. 2004a. Illumination of cryptic species boundaries in long-tailed shrew tenrecs (Mammalia: Tenrecidae; *Microgale*), with new insights into geographic variation and distributional constraints. *Biological Journal of the Linnean Society* 83:1–22.
- OLSON, L. E., E. J. SARGIS, AND R. D. MARTIN. 2004b. Phylogenetic relationships among treeshrews (Scandentia): a review and critique of the morphological evidence. *Journal of Mammalian Evolution* 11:49–71.
- OLSON, L. E., E. J. SARGIS, AND R. D. MARTIN. 2005. Intraordinal phylogenetics of treeshrews (Mammalia: Scandentia) based on evidence from the mitochondrial 12S rRNA gene. *Molecular Phylogenetics and Evolution* 35:656–673.
- RAFFLES, T. S. 1821. Descriptive catalogue of a zoological collection, made on account of the honourable East India Company, in the island of Sumatra and its vicinity, under the direction of Sir Thomas Stamford Raffles, Lieutenant-Governor of Fort Marlborough; with additional notices illustrative of the natural history of those countries. *Transactions of the Linnean Society of London* 13:239–274.
- ROBERTS, T. E., H. C. LANIER, E. J. SARGIS, AND L. E. OLSON. 2011. Molecular phylogeny of treeshrews (Mammalia: Scandentia) and the timescale of diversification in Southeast Asia. *Molecular Phylogenetics and Evolution* 60:358–372.
- SARGIS, E. J. 2002a. Functional morphology of the forelimb of tupaiids (Mammalia, Scandentia) and its phylogenetic implications. *Journal of Morphology* 253:10–42.

- SARGIS, E. J. 2002b. Functional morphology of the hindlimb of tupaiids (Mammalia, Scandentia) and its phylogenetic implications. *Journal of Morphology* 254:149–185.
- SARGIS, E. J. 2002c. A multivariate analysis of the postcranium of tree shrews (Scandentia, Tupaiidae) and its taxonomic implications. *Mammalia* 66:579–598.
- SARGIS, E. J., K. K. CAMPBELL, AND L. E. OLSON. In press. Taxonomic boundaries and craniometric variation in the treeshrews (Scandentia, Tupaiidae) from the Palawan faunal region. *Journal of Mammalian Evolution* DOI 10.1007/s10914-013-9229-2.
- SARGIS, E. J., N. WOODMAN, A. T. REESE, AND L. E. OLSON. 2013. Using hand proportions to test taxonomic boundaries within the *Tupaia glis* species complex (Scandentia, Tupaiidae). *Journal of Mammalogy* 94:183–201.
- SCHLICK-STEINER, B. C., B. SEIFERT, C. STAUFFER, E. CHRISTIAN, R. H. CROZIER, AND F. M. STEINER. 2007. Without morphology, cryptic species stay in taxonomic crypsis following discovery. *Trends in Ecology and Evolution* 22:391–392.
- THOMAS, O. 1895. On some mammals collected by Dr. E. Modigliani in Sipora, Mentawai Islands. *Annali. Museo Civico de Storia Naturale Genoa ser. 2* 14:661–672.
- WILSON, D. E. 1993. Order Scandentia. Pp. 131–133 in *Mammal species of the world: a taxonomic and geographic reference*. 2nd ed. (D. E. Wilson and D. M. Reeder, eds.). Smithsonian Institution Press, Washington, D.C.
- WOODMAN, N. 2010. Two new species of shrews (Soricidae) from the western highlands of Guatemala. *Journal of Mammalogy* 91:566–579.
- WOODMAN, N. 2011. Patterns of morphological variation amongst semifossorial shrews in the highlands of Guatemala, with the description of a new species (Mammalia, Soricomorpha, Soricidae). *Zoological Journal of the Linnean Society* 163:1267–1288.
- WOODMAN, N., AND J. J. P. MORGAN. 2005. Skeletal morphology of the forefoot in shrews (Mammalia: Soricidae) of the genus *Cryptotis*, as revealed by digital X-rays. *Journal of Morphology* 266:60–73.
- WOODMAN, N., AND R. B. STEPHENS. 2010. At the foot of the shrew: manus morphology distinguishes closely related *Cryptotis goodwini* and *Cryptotis griseoventris* (Mammalia: Soricidae) in Central America. *Biological Journal of the Linnean Society* 99:118–134.
- (MVZ); Naturhistorisches Museum Basel (NMB); Naturhistorisches Museum Wien, Vienna (NMW); Nationaal Natuurhistorisch Museum, Leiden (RMNH); United States National Museum of Natural History, Smithsonian Institution, Washington, DC (USNM); Museum für Naturkunde, Berlin (ZMB); Zoologisk Museum University of Copenhagen (ZMUC). See Sargis et al. (2013) for subspecies designations. All 35 *T. glis* specimens were used for analyses of both the skull and manus; specimens of the other 3 species used in both analyses are indicated with an asterisk (*).
- Tupaia ferruginea* ($n = 64$).—INDONESIA: Sumatra: no locality (MCZ 6276; ZMB 11460, 87172; ZMUC 19); Bencoolen [Bengkulu] (type locality; BMNH 79.11.21.573—holotype); Rimbo Pengadang (Lebong), Bengkulu [Bengkulu] (RMNH 12602); Tarussan Bay (USNM 141074*); Loh Sidoh Bay (USNM 114152*, 114153*); Aru Bay (FMNH 43835; USNM 143329*, 143333*); Tapanuli Bay (USNM 114548*, 114549*, 114553); Langsa, Atjeh [Aceh] (RMNH 34183, 34185); Perlak, Atjeh [Aceh] (FMNH 47123–47125; RMNH 34163, 34165–34167, 34169, 34171–34177, 34180–34182, 44290; USNM 257593*, 257594*, 257595*, 257596*); Little Siak River (USNM 144204*, 144205, 144209*); Indragiri (NMB 2992, 10005); Indragiri River (USNM 174610); Batu Islands, Tanahbala (USNM 121752); Lower Langkat (BMNH 4.4.1.4, 4.6.9.1; NMB 10004); Lampongs [Lampung] (RMNH 15634–15637, 15639, 15640); Giesting, Lampoengs (RMNH 34186); Panhalan [Pangkalan] Brandan (ZMB 33979); Padangse Bovenlanden (Haut Padang; RMNH 36112); Ketambe Research Station, Leuser National Park, 400 m, Aceh (MVZ 192187); Seolah Dras, Korinchi Valley (BMNH 19.11.5.17); Deli (LACM 52185); Pajo (BMNH 79.6.28.15); Paja, Bahong, Deli, Langsa (NMW 4540).
- Tupaia chrysogaster* ($n = 25$).—INDONESIA: Pagai Utara (North Pagai) Island (type locality) (AMNH 103093, 103094, 103097, 103098, 103100, 103102, 103103, 103106, 103316; RMNH 34235; USNM 121571*, 121572—holotype, 121573*, 121575*); Pagai Selatan (South Pagai) Island (USNM 121577*, 121579*); Sipora Island (BMNH 28.11.2.4; USNM 252330*–252333*, 252334, 252335*, 252337*, 252338*).
- Tupaia glis* ($n = 35$).—INDONESIA: Siberut Island (USNM 252328, 252329). Kepulauan Riau: Riau Archipelago; Djemadja Island (USNM 101741, 101742); Batam Island (USNM 142152); Bintang Island (USNM 115607). Lingga Archipelago, Singkep Island (USNM 113147, 113149). MALAYSIA: Kedah: Pulo Langkawi (USNM 104353, 123901). Pahang: Pekan District, Tioman Island (USNM 101746, 104973–104976, 487932–487934, 487936–487938). SINGAPORE: (USNM 124317). THAILAND: Satun: Butang Islands, Pulo Adang (USNM 104354); Surat Thani: Koh Phangan Island (USNM 256882); Pulo Terutau (USNM 123981, 123982, 123985, 123987). Trang: Trang (USNM 83254, 83257, 83477); Kao Sai Dao (USNM 258927); Kao Chong (USNM 258928); Telibon Island (USNM 83256). Nakhon Si Thammarat: Seechol (USNM 255754).
- Tupaia hypochrysa* ($n = 8$).—INDONESIA: Java: no locality (BMNH 86.7.2.12*—holotype; RMNH 36108, 36116; ZMB 633); Tjerimai, 1000 m (AMNH 101718*); Tosari (RMNH 12657); West Java, Tjibodas (BMNH 54.63*); Gunung Salak (USNM 154599*).

Submitted 8 February 2013. Accepted 15 March 2013.

Associate Editor was Ryan W. Norris.

APPENDIX I

Specimens examined

Specimens from the following institutions (with abbreviations) were included in this study: American Museum of Natural History, New York (AMNH); The Natural History Museum, London (BMNH); Field Museum of Natural History, Chicago (FMNH); Los Angeles County Museum of Natural History, Los Angeles (LACM); Museum of Comparative Zoology at Harvard University, Cambridge (MCZ); Museum of Vertebrate Zoology at University of California, Berkeley